Material Considerations in Plastic Design

Etude des matériaux de type plastique

Materialerwägungen für den plastischen Entwurf

PETER F. ADAMS
A.M. ASCE, Associate Professor of Civil Engineering, University of Alberta, Edmonton, Alberta

THEODORE V. GALAMBOS
M. ASCE, Professor of Civil Engineering, Washington University, St. Louis, Missouri

Introduction

This report discusses the influence of the strain-hardening characteristics of steel on the inelastic behavior of a beam. In particular, the ability of such a member to redistribute bending moments in the inelastic range is investigated. This study was initiated as part of a program to develop plastic design rules for high strength, low alloy steels. These steel types have characteristics which are somewhat different than those observed for the low-carbon steels [1]. In addition, it has been observed that the rotary cold-straightening process may change the properties from those of the virgin material [2, 3].

The basis of the "simple plastic theory" is the assumption that moment redistribution can occur so that the plastic moment capacity, M_p, is reached and held at a number of locations and thus the structure can fail as a mechanism [4]. The moment-curvature relationship is assumed to be ideally elastic-plastic [2]. The inelastic rotations are therefore, concentrated at discrete points (hinges). As the structure is loaded and the plastic moment is reached at successive hinge locations, discrete reductions in stiffness replace the gradual deterioration which occurs in an actual structure. This simplified treatment provides a good indication of the overall behavior of the structure and a convenient means of determining the maximum load [4].

To study the local behavior in the hinge areas, and to determine the actual deformation capacity of a member, an analysis must account for the strain

hardening properties of the material and for the real curvature distribution along the length of the member [5].

This report presents the results of such an analysis. The structure is assumed to consist of a material with the stress-strain ($\sigma - \epsilon$) relationship shown in Fig. 1. The yield stress is denoted as σ_y and E represents the modulus of elasticity, in Fig. 1. The strain hardening modulus is denoted by E_{st}. The yield strain and the strain at the onset of strain hardening are ϵ_y and ϵ_{st}, respectively. The effect of the material characteristics is studied by varying the values of E_{st} and/or ϵ_{st}. The results are discussed with the object of determining those factors which influence the ability of the structure to redistribute bending moment.

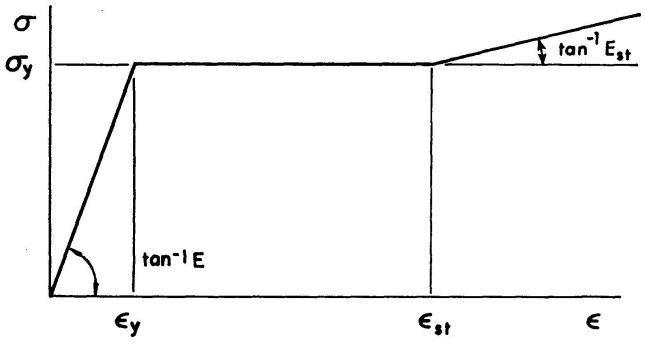

Fig. 1. Stress-strain diagram.

The rotary straightening process is performed by cold bending the rolled section about its weak axis back and forth between two sets of heavy rolls. Such cold working induces residual stresses and it may alter the effective strain-hardening properties of the material. The effect of rotarizing on the material properties is illustrated on an analytical model. The predicted material properties are compared with those measured on tensile coupons cut from rotarized sections [3].

Analysis of Three Span Beam

The model chosen for the investigation is the symmetrical three span beam shown in Fig. 2a. The member has a center span of length, L, side spans of length, αL, and is loaded with a concentrated load, P, at the mid-point of the centre span. The beam is composed of material possessing the characteristics shown by the $\sigma - \epsilon$ curve of Fig. 1. The model is relatively simple to analyze and the results illustrate clearly the relative influence of the stress-strain characteristics. The analysis was performed on a beam having $\alpha = 1.0$.

If the cross-section is assumed to be composed of two infinitely thin flanges separated by the depth of the cross-section, d, and the effect of residual stress is neglected, the moment-curvature ($M - \phi$) relationship is that shown in Fig. 3 [6]. In this figure M is the full plastic moment and I is the major axis

moment of inertia of the cross-section. The curvature corresponding to the attainment of M_p is ϕ_p and that at the initiation of strain hardening is ϕ_{st}. The $M-\phi$ relationship shown in Fig. 3 is based on the assumption that instability of the cross-section does not occur.

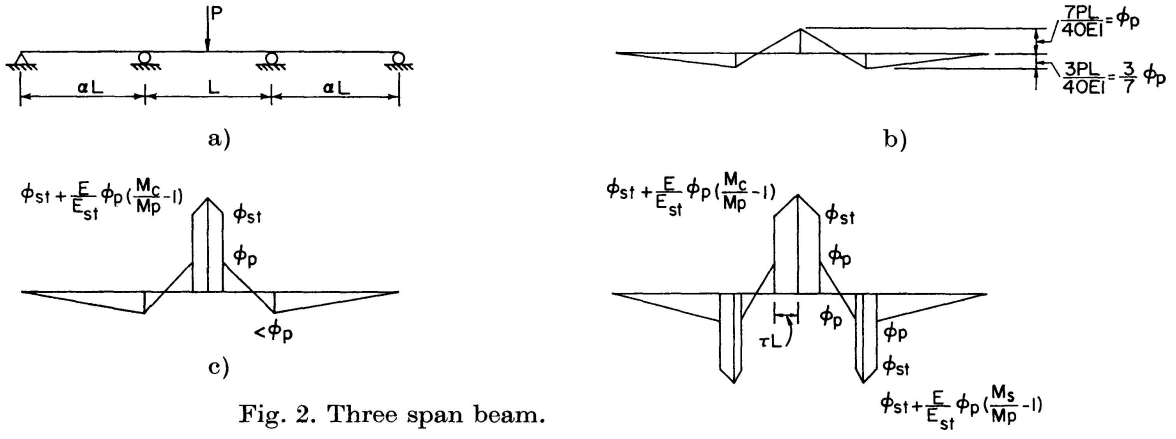

Fig. 2. Three span beam.

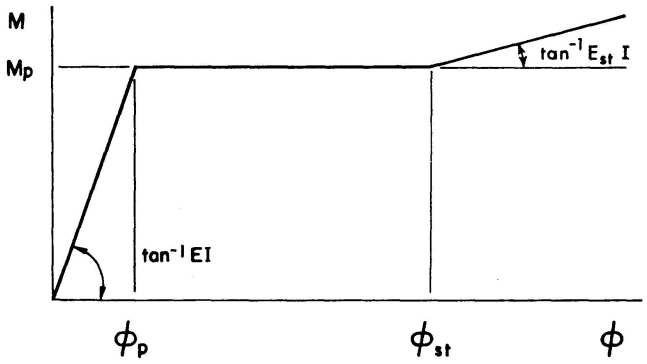

Fig. 3. Moment-curvature.

The behavior of the beam will be described with reference to Fig. 2. The curvature distribution along the length of the member at the hypothetical elastic limit is shown in Fig. 2b. At this stage of loading the curvature at the load point is equal to ϕ_P. As the load is increased, the moment at the load point, M_c exceeds M_P and the yielded zone spreads from the mid-span section along the length of the member. The curvature distribution at this stage is shown in Fig. 2c. If the load is increased further, the moments at the interior supports, M_s, also exceed M_P and yielded zones begin to spread from the supports. The corresponding curvature distribution is shown in Fig. 2d.

The in-plane load-deflection behavior of the beam will be traced using the $M-\phi$ curve of Fig. 3. The curvature distributions shown in Fig. 2 are non-dimensionalized in such a way that the only numerical data necessary for the analysis are the ratios of E/E_{st} and ϵ_{st}/ϵ_y [3]. The effect of the material characteristics will be examined by varying these two ratios.

An analysis similar to that presented here was presented by HORNE [7]. An analysis which considered, in addition, the effects of gradual yielding and residual stress was given by LAY and SMITH [8]. Horne considered only the

effect of the strain hardening modulus on the equalization of moments at hinge locations; Lay and Smith showed that strain hardening was necessary for moment redistribution. The present paper shows the effects of the variation of E_{st} and ϵ_{st}, varying over the practical range of these properties, on the internal force distribution. The investigation also shows the variation of the yielded length at the load point, the load point deflection and the maximum strain over the same range of the material characteristics.

The primary factor which limits the rotation capacity in a braced beam under moment gradient is local buckling of the compression flange [9, 10]. This is due to the large strains present in portions of the member adjacent to the plastic hinges. It has been shown that to delay the occurrence of local buckling until the optimum rotation capacity has been obtained, the flange width-to-thickness (b/t) ratio must be limited approximately to:

$$\frac{b}{t} = 2\sqrt{\frac{G'}{\sigma_y}}, \tag{1}$$

where G' is the torsional rigidity in the strain hardening range, given by:

$$G' = \frac{2\,G}{1+\frac{E}{4\,E_{st}}\,\frac{1}{(1+\mu)}}. \tag{2}$$

In Eq. (2), G is the elastic torsional rigidity and μ is Poisson's ratio [11].

For ASTM-A 36 or A 441 steel, which has not been cold worked, E_{st} varies approximately from $E/35$ to $E/45$. The limiting b/t ratio for A 36 steel ($\sigma_y =$ 36 ksi) is 17 (from Eq. (1)), and for A 441 steel, ($\sigma_y = 50$ ksi) the ratio is 14 if $E_{st} = E/45$. If, however, E_{st} were only $E/450$, which might represent a lower bound for steel which has been yielded during the cold-straightening process, the corresponding limits of b/t would be 5.5 and 4.7.

Thus to ensure reasonable limits for the flange plate geometry in sections used for plastic design, the value of E_{st} should be as large as possible. This is particularly important with the high strength steels because a higher value of σ_y results in a lower limiting b/t ratio.

Results of Analysis

Computations have been performed for three ratios of E/E_{st}; 45, 160 and 450; and five ratios of ϵ_{st}/ϵ_y; 1, 3, 6, 12 and 20. The values of E/E_{st} and ϵ_{st}/ϵ_y were chosen to represent the limits of behavior for structural steel both in the virgin condition and after cold working. Throughout the studies in this section the strain hardening modulus is assumed to be a constant.

The increase in bending moment with increased load at two critical locations in the beam is shown in Fig. 4. These plots trace the process of moment redistribution. The load P, non-dimensionalized as P/P_p, is plotted on the

vertical axis, where P_p is the load predicted by simple plastic theory ($P_p = 8M_p/L$). The bending moments at the support and at the load-point, M, are plotted on the horizontal axis. The moments are non-dimensionalized as M/M_p. The predictions given by an elastic-plastic analysis are shown as the dashed lines [6]. As opposed to the idealized elastic-plastic prediction, consideration of the strain hardening properties of the material results in an increase in the load-point moment once yielding has been initiated at this point. At $P/P_p = 1.0$, the load-point moment is well above M_p while that over the interior support is below M_p.

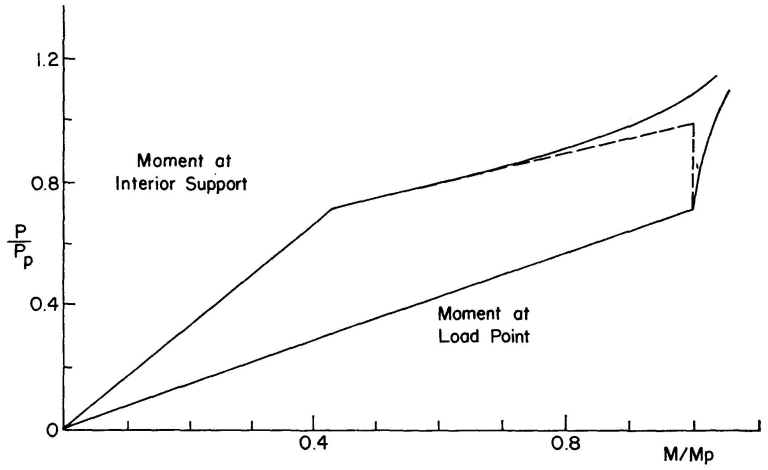

Fig. 4. Load-moment curves.

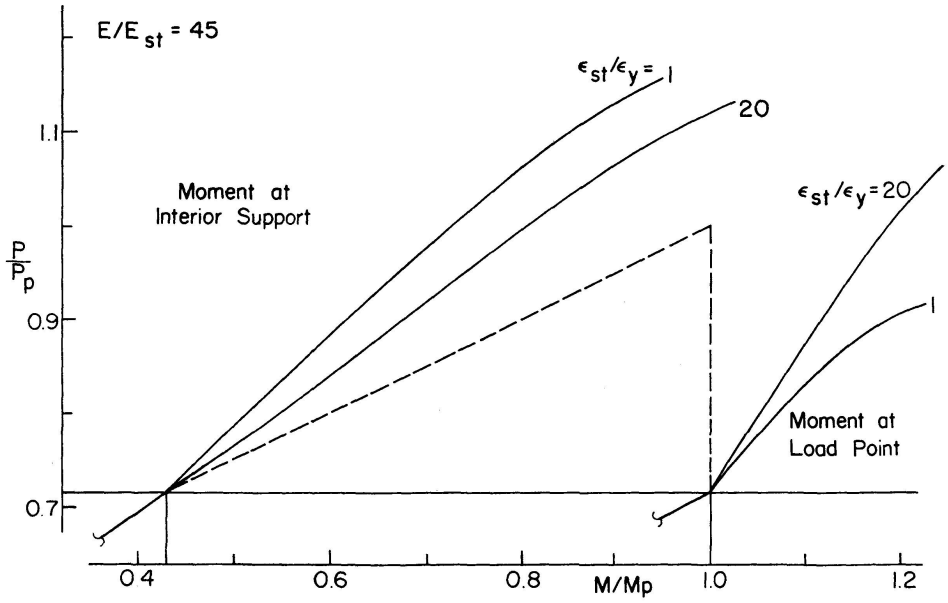

Fig. 5. Load-moment curves-varying ϵ_{st}/ϵ_y.

The region of interest in Fig. 4 is shown in detail in Fig. 5. In Fig. 5 the curves are plotted for $E/E_{st} = 45$ and for two ratios of ϵ_{st}/ϵ_y; 1 and 20. From Fig. 5 it can be seen that the material with $\epsilon_{st}/\epsilon_y = 20$ approaches more closely the elastic-plastic prediction than the material with $\epsilon_{st}/\epsilon_y = 1$. The same trend

was observed when ϵ_{st}/ϵ_y was held constant and E/E_{st} increased. This result is as expected since the response of an elastic-plastic material could be obtained by allowing ϵ_{st}/ϵ_y or E/E_{st} to approach infinity.

Fig. 6 summarizes the results of the computations by plotting the moment under the load M_c/M_p against the ratio of ϵ_{st}/ϵ_y. The graphs are plotted at the attainment of the simple plastic theory load, $P/P_p = 1.0$. The plots show that for materials with small values of ϵ_{st}/ϵ_y or E/E_{st} the maximum moment at $P/P_p = 1.0$ is larger. The maximum value of the moment under the hinge point is $1.27\,M_p$ for a material with $\epsilon_{st}/\epsilon_y = 1$ and $E/E_{st} = 45$. The maximum moment decreases as the value of ϵ_{st}/ϵ_y and/or E/E_{st} increases and it eventually approaches M_p asymptotically.

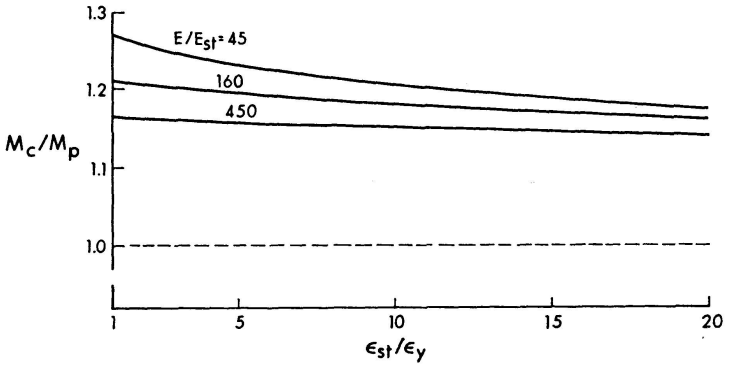

Fig. 6. Maximum moment ($P/P_p = 1.0$).

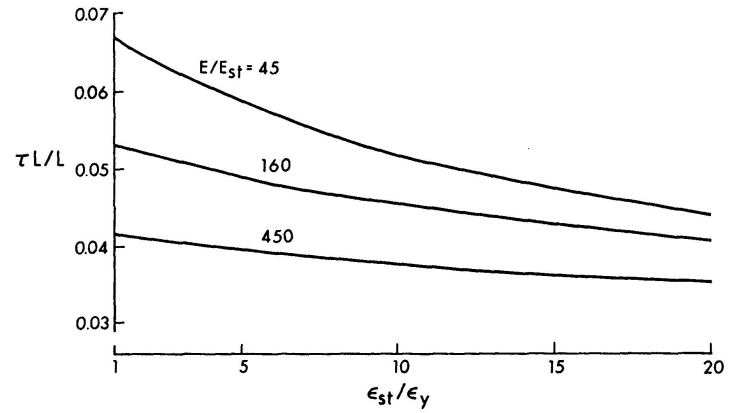

Fig. 7. Yielded length ($P/P_p = 1.0$).

When M_p has been reached under the load, the zone of large curvatures shown in Fig. 2c must spread from the load point along the length of the beam. Simultaneously, the moment at this location, M_c, increases above M_p. Once the yielded length of the beam, τL, has reached a sufficient magnitude for a local buckle to form, the response of the member can no longer be predicted and its useful life is assumed to be terminated. The value of τL at $P/P_p = 1.0$ is thus a critical property and is plotted in Fig. 7 for the materials considered.

In Fig. 7, ϵ_{st}/ϵ_y is plotted against the yielded length, $\tau L/L$. Those materials which have larger values of ϵ_{st}/ϵ_y, will develop shorter yielded lengths at the simple plastic load level ($P/P_p = 1.0$). Thus, these materials have a larger

rotation capacity up to the formation of a local buckle. The same trend was evident for those materials having larger values of E/E_{st} [3].

For wide flange shapes of compact cross-section, the wave-length of a local buckle is $2\,L_{lb}$ [11] where:

$$2\,L_{lb} = 1.42\left(\frac{b\,t}{dw}\right)\left(\frac{A_w}{A_f}\right)^{1/4} d. \tag{3}$$

At the initiation of local buckling then:

$$\tau_{lb} = \frac{2\,L_{lb}}{L} = 1.42\left(\frac{b\,t}{dw}\right)\left(\frac{A_w}{A_f}\right)^{1/4}\left(\frac{d}{L}\right). \tag{4}$$

In Eqs. (3) and (4), b and t denote the flange width and thickness while d and w denote the total depth of the section and the web thickness, respectively. The area of one flange is $A_f = b\,t$ and the web area $A_w = w\,(d-2\,t)$.

For wide flange sections commonly used as beams, the cross-sectional properties pertinent to local buckling have been tabulated [12]. For these sections the value of $\left(\frac{b\,t}{dw}\right)\left(\frac{A_w}{A_f}\right)^{1/4}$ varies from 0.50 to 0.95. Assuming that $10 \leqq L/D \leqq 30$. The resulting value of τ_{lb} varies from 0.024 to 0.135. From Fig. 7, the value of τ_{lb} required to ensure that the load can reach P_p varies from 0.044 to 0.068. Members having relatively low values of $\left(\frac{b\,t}{dw}\right)\left(\frac{A_w}{A_f}\right)$ combined with high L/d ratios may local buckle before reaching the load predicted by simple plastic theory. Recent tests have shown that rolled wide-flange members have significant post local buckling capacity [13]. Thus, although local buckling may occur at loads below $P/P_p = 1.0$, it is highly unlikely that a compact section member will fail to reach this load.

From the above considerations, it appears, that ideally a steel should have as large a value of E_{st} as possible to provide better resistance to local buckling, and as large a value of ϵ_{st} as possible to provide for smaller moments at plastic hinge locations and to ensure that the yielded length extends over as short a length as possible [14].

Theses conclusions must be tempered by a consideration of the deflections and strains, which should be held to as small a value as possible to restrict second order effects. In Fig. 8 the variation of the in-plane deflection at the load-point, v, non-dimensionalized as $\frac{v}{L}\frac{1}{\epsilon_y}\frac{d}{L}$ (where d is the depth of the cross-section) is examined.

It can be seen that a beam composed of a material with a large value of ϵ_{st}/ϵ_y will deflect more than a corresponding member composed of material having a smaller value of ϵ_{st}/ϵ_y. The same trend is evident with respect to the value of E/E_{st}. For very large values of these two parameters the deflection at $P/P_p = 1.0$ approaches that predicted by simple plastic theory.

For structural steel having $E/E_{st} = 45$ and $\epsilon_{st}/\epsilon_y = 12$ (the normally accepted values for A 36 steel) the simple plastic theory would over-estimate the deflec-

tions by 46%. This is of little significance as, in most cases, the member will be within the elastic range under working loads. It does, however, point out the fact that the deflections predicted by plastic theory may be excessively conservative if reduced linearly to the working load level.

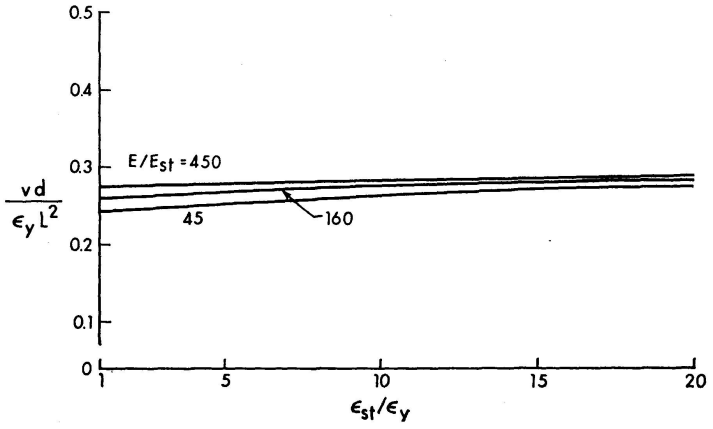

Fig. 8. Deflection ($P/P_p = 1.0$).

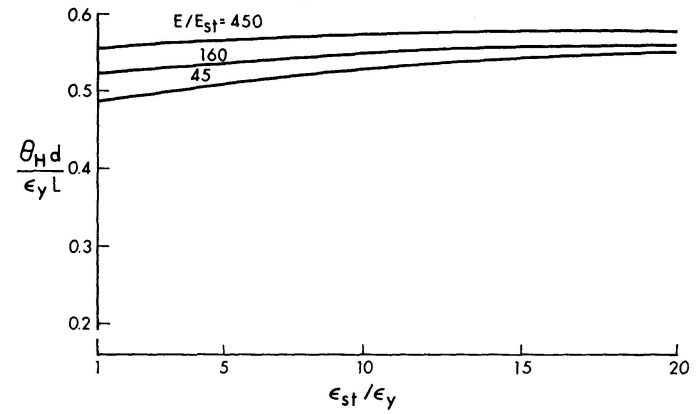

Fig. 9. Hinge rotation ($P/P_p = 1.0$).

Fig. 9 plots the hinge rotation, θ_H, required to reach $P/P_p = 1.0$. The hinge rotation is non-dimensionalized as $\theta_H/\phi_p L$ and plotted against ϵ_{st}/ϵ_y. Trends similar to those discussed in connection with Fig. 8 are evident in Fig. 9. An analysis based on an ideal elastic-plastic $M-\phi$ curve over estimates the hinge rotation required to reach $P/P_p = 1.0$. One undesirable consequence of this is that any structural limitation (bracing spacing, plate geometry, etc.), which is based on required rotations calculated on the basis of an elastic-plastic analysis, may be unduly conservative.

The maximum strains, ϵ_{max}, occuring under the load point at $P/P_p = 1.0$ are plotted in Fig. 10. In this figure $\epsilon_{max}/\epsilon_y$ is plotted versus ϵ_{st}/ϵ_y. For materials with larger values of ϵ_{st}/ϵ_y and/or E/E_{st} the maximum strain is increased. In no case does the maximum strain exceed $90\,\epsilon_y$, thus the danger of failure by fracture at loads below $P/P_p = 1.0$ does not exist.

It has been argued that materials which do not posess strain hardening properties will not redistribute moments in the inelastic range [8, 15]. However, all structural metals do exhibit strain hardening to some extent, and it has

been shown that the primary effect of the reduced value of E_{st} is the lowered resistance to local buckling [9].

It appears that the stress-strain characteristics of the structural steels make them well suited for their role in plastic design. The relatively large values of E_{st} (900 ksi for ASTM-A 36, 750 ksi for A 441) result in acceptable limits on the flange geometry to prevent premature local buckling [1, 16]. On the other hand the jump in strain at the yield stress (approximately $12\,\epsilon_y$) provides a large rotation capacity while resulting [17] in a relatively short yielded length.

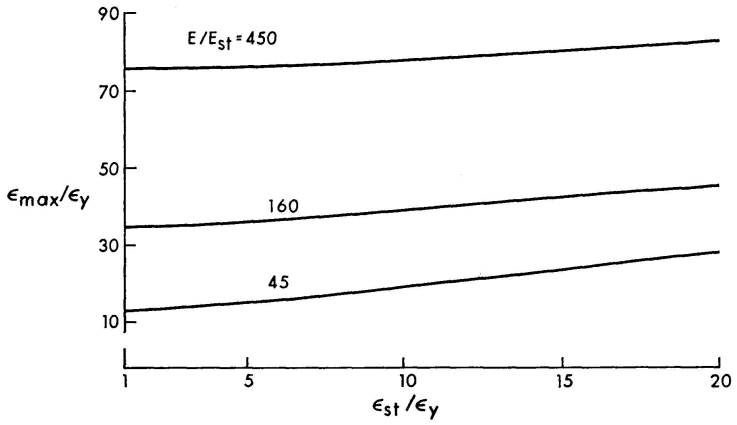

Fig. 10. Maximum strain ($P/P_p = 1.0$).

The conclusions above are based on a very simple model, however, in a relative sense, they are valid also for more complex structures. Presently, plastically designed structures are proportioned to provide the maximum possible rotation capacity; it is then assumed that this capacity will be sufficient to allow the structure to reach P_p.

The strain hardening porperties E_{st} and ϵ_{st} appear to be more scattered than the values of E and σ_y. It is, therefore, gratifying to note that even relatively large variations in E_{st} and ϵ_{st} do not produce grossly undesirable effects.

The Influence of Cold Bending

The stress-strain relationship of the material, after rolling and cooling, has normally been taken as the basis for predicting member behavior. The influence of those portions of the member which had been locally yielded when the member was cold bent (gagged), to improve straightness or during fabrication, was neglected [18]. Since the affected areas form only a small proportion of the total length of the member, the neglect of this influence is justified.

In recent years the use of the rotary straightener by steel mills has increased. Although it is presently limited to the smaller sections (one approximate rule of thumb is that the weak axis section modulus be less than 15) it appears that its use will be extended to larger sections.

Essentially, the rotary straightener consists of a series of heavy rolls spaced

as shown in Fig. 11 and used to bend the section about the weak axis. The rolls are arranged so that they bear directly on the flange-to-web junctions of the beam and subject it to two complete cycles of curvature reversal; rolls No. 4 to 7 being the active, or load producing rolls. The member is fed continuously into the roller arrangement, guided by rolls No. 1, 2 and 3. Roll No. 4 is placed in a lowered position relative to the first three. The difference in elevation may vary from a fraction of an inch to several inches, depending on the size of the member, but is enough to produce a significant permanent curvature in the beam. Roll No. 5 then picks up the end of the member and reverses the direction of the curvature. The permanent curvature produced by

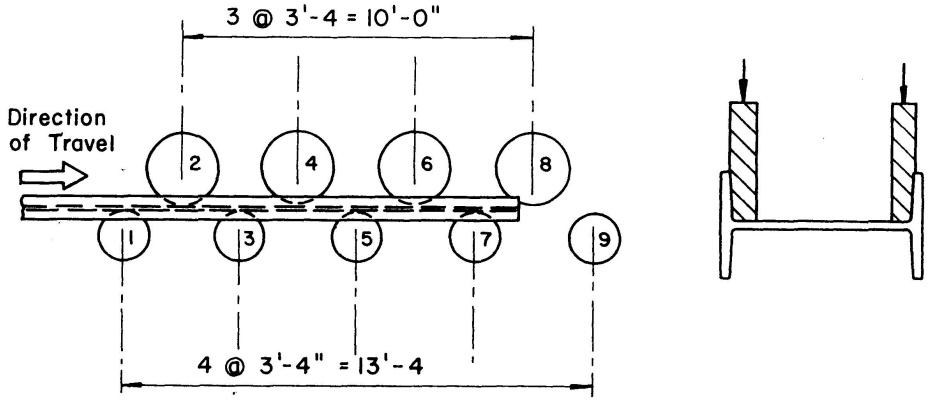

Fig. 11. Rotarizing process.

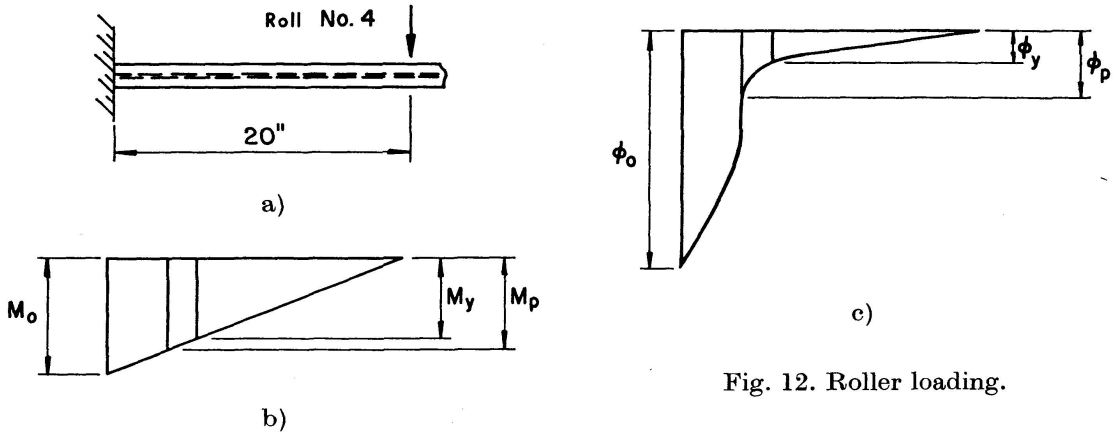

Fig. 12. Roller loading.

this roll is approximately one-half that produced by roll No. 4. Rolls No. 6 and 7 repeat the process with correspondingly reduced magnitudes of curvature, and the remainder of the rolls act primarily as guides. The entire process is one of trial and error. The first lengths of a given cross-section are rotarized with trial settings of the rolls. If the member is straightened in a satisfactory manner the remainder of the lengths are processed in the same way; if not, new settings are tried and the process repeated. During the process any initial curvatures virtually disappear and the final product is almost uniformly straight.

The loading situation at the time roll No. 4 engages the forward end of the beam is shown (approximately) in Fig. 12a. The corresponding bending moment distribution is shown in Fig. 12b, and the curvature distribution in Fig. 12c. In Fig. 12, M_y is the moment corresponding to the initiation of yielding in the extreme fibres of the cross-section and M_0 is the maximum moment on the member. The corresponding curvatures are ϕ_y and ϕ_0. The complete length of the beam is subjected to the applied curvature ϕ_0 as it is guided under roll No. 4 and is then unloaded elastically after passing this roll. A smaller curvature, applied in the reverse sense, is then induced by the action of roll No. 5 and so on. In order to compute the influence of this process on the member, the material behaviour under reversed loading must first be evaluated.

The material behavior postulated by CHAJES et al. [19] and used in a modified form by LAY [20) will be adopted. This behavior is illustrated in Fig. 13

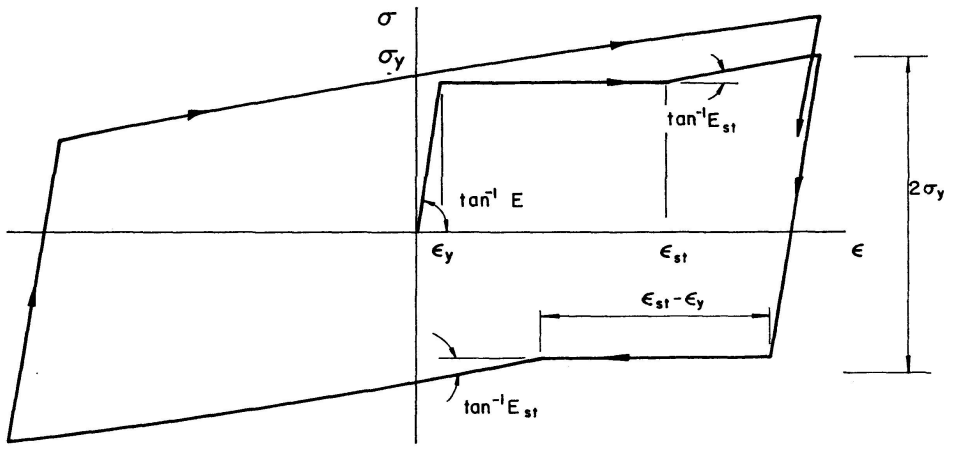

Fig. 13. Stress-strain diagram.

and accounts for the unique stress-strain characteristics of the structural steels as well as (approximately) the Bauschinger effect [21]. To gain some insight into the influence of the reversed strains on the material properties, the linear strain-hardening range assumed by Lay has been replaced with a parabolic curve fitted to the initial modulus E_{st} at the initiation of strain hardening and to the ultimate stress and strain [3]. This takes into account the deterioration of E_{st} in the strain-hardening region.

Using these assumptions it is possible to trace the behaviour of the material through the strain reversals involved in the rotarizing process. In order to do this a sequence of applied curvatures has been selected as shown in Fig. 14. The initial curvature, ϕ_1, is $20\,\phi_y$ where ϕ_y is the curvature corresponding to the attainment of the yield strain at the flange tips. This is not completely arbitrary as it results in an approximate value for the deflection under the roll No. 4 of 1 inch, which seems reasonable. The curvature is then reversed twice; ϕ_2 being equal to $10\,\phi_y$ and ϕ_3 equal to $5\,\phi_y$. The final applied curvature

ϕ_4 is taken as $1.7\,\phi_y$ from a trial and error process which will be described below. This value is required to ensure that the final configuration results in no residual curvature on completion of the process. At this point however, there will be residual strains in the flanges, which are a result of the inelastic strains induced by the reversed bending being superimposed on those which are induced during cooling. Only the flange is considered in the analysis, the web is relatively unaffected.

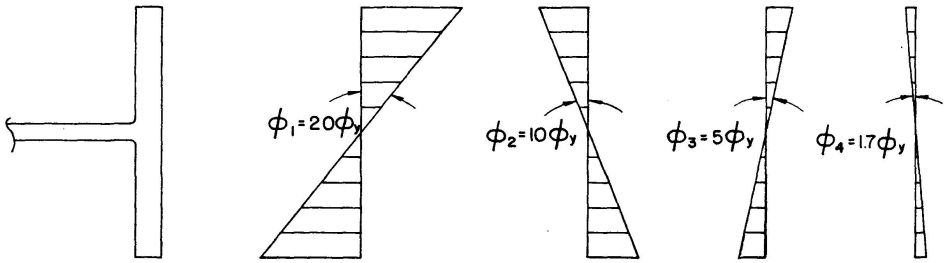

Fig. 14. Sequence of curvatures.

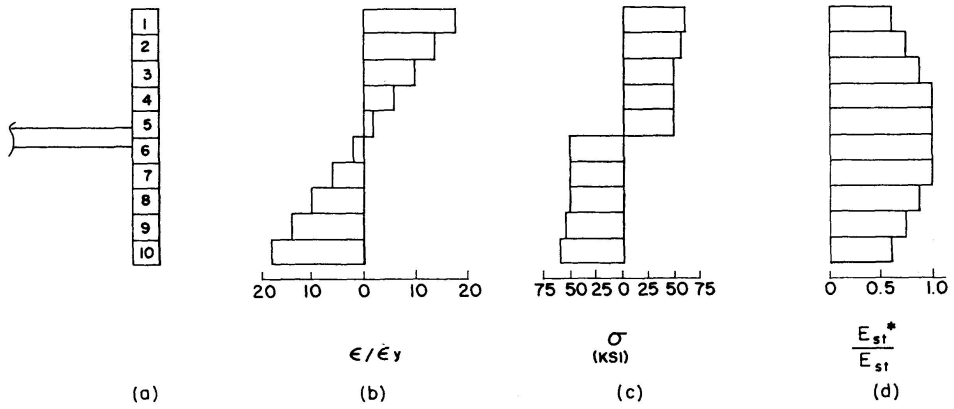

Fig. 15. Integration process.

To determine the influence of this process on the material, an approximate analysis was used. The flange width was divided into ten elements as shown in Fig. 15a and the strains induced by the applied curvatures computed at the centroid of each element. For the first applied curvature, ϕ_1, the strains in each element, ϵ, non-dimensionalized as ϵ/ϵ_y, are shown in Fig. 15b and the corresponding stresses, σ, in Fig. 15c. The stresses were calculated on the basis of a flange width of 6 inches and thickness of 0.44 inches and for material having the characteristics of A 441 steel.

By integrating the stresses over the cross-section, the applied moment required to produce a curvature of $20\,\phi_y$ can be computed. This process is repeated for the reversals of curvature specified in Fig. 14 and for the final elastic unloading. This final unloading should produce a zero net curvature for zero applied moment. Thus the final applied curvature, ϕ_4, was adjusted to achieve this end.

During the cold bending process, each fibre of the material is assumed to behave in a manner similar to that depicted in Fig. 13. The cross-section at the end of the process is in equilibrium and has a negligible residual curvature, however, each fibre has at some stage been subjected to a longitudinal strain that may be in the order of 20 or 30 ϵ_y. Thus, the fibre, when strained in service due to the action of a superimposed external load, may behave in a bilinear manner with a reduced strain hardening modulus. The reduction is because of the deterioration of the modulus with increased strain.

The residual stresses which result from the rotarizing process have been predicted and these predicted values compared with measured values [3]. The trends in residual stress distribution agree fairly well although the numerical values are not in close agreement. Of much greater importance is the effect on the stiffness of the material in the strain-hardening range. Fig. 15d shows the effective strain-hardening modulus, E_{st} plotted as a fraction of the initial modulus for the section used in the example. These values would result from the strain reversals shown in Fig. 14. The inelastic stiffness of the section is somewhat reduced by the process, but much more work remains to be done to determine fully the influence of the rotarizing process on the behaviour of plastically designed members.

The results of tension tests performed on specimens cut from rotarized members tend to confirm these trends [2]. The tests used in this comparison are those performed on specimens cut from 12 B 16.5 beams of A 36 steel. The flange width is 4 inches. The specimens were milled from coupons located in the flange between the tip of the flange and the centre line of the web. If the rotarizing sequence described above is typical, then the material near the flange tip has undergone a series of strain reversals similar to that traced for the tip of the section in Fig. 14 while the material near the web has remained almost completely elastic.

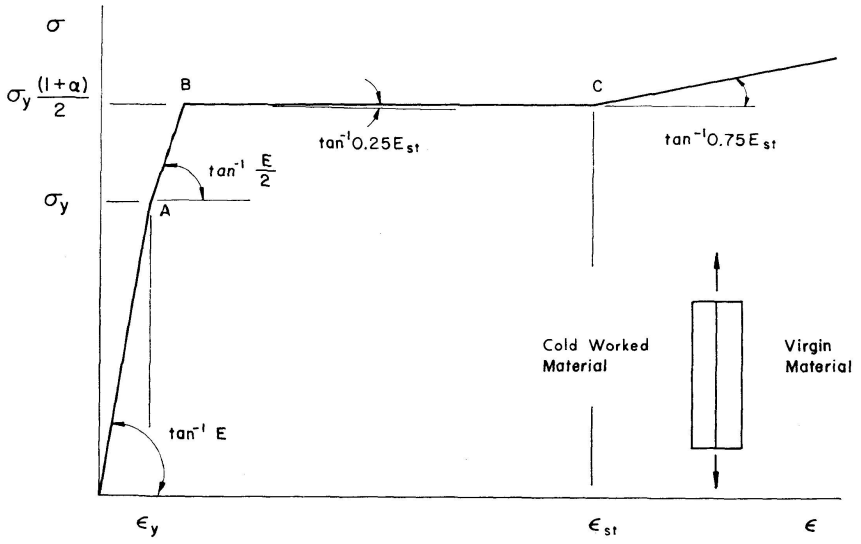

Fig. 16. Tension specimen model.

To simulate this case a model is postulated as shown in the inset to Fig. 16 in which half the width of the specimen is noted as cold worked and is assumed to have been subjected to the rotarizing sequence. The other half is noted as the virgin material.

As the model is loaded in tension, the behaviour will be elastic until the applied stress reaches the yield stress of the virgin material, σ_y. This occurs at point A in Fig. 16. At this point the virgin material will accept further strain with no increase in load, however, the cold worked material will behave in an elastic manner up to a stress of $\alpha\,\sigma_y$, the increased yield stress of the cold worked material. Thus the model deforms from A to B in Fig. 16 with an effective modulus of $E/2$. At point B the increased yield stress of the cold worked material is reached. To achieve any further deformation the cold worked material must be subjected to an increased stress. Due to the reduction in stiffness, as evidenced by Fig. 15d, this increased stress will be small. At point C the strain-hardening hardening strain of the virgin material is reached and further deformation now requires a distinct increase in stress. The effective modulus is approximately three-quarters of that for the virgin material.

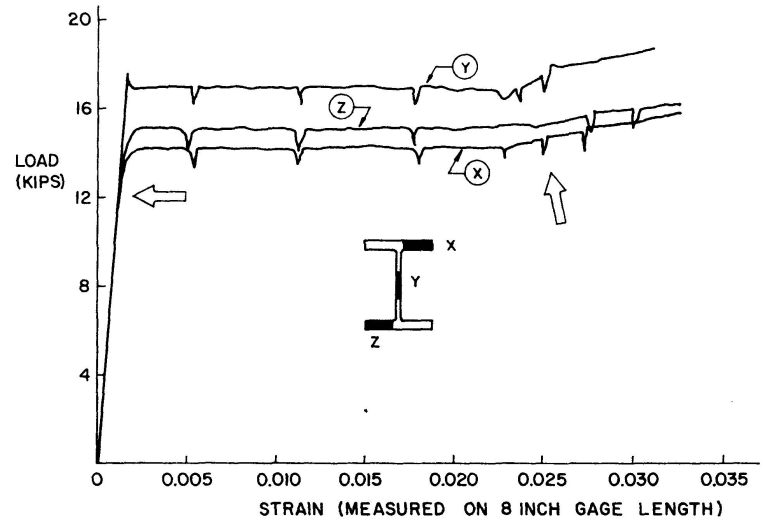

Fig. 17. Load-strain curves.

The strain-hardening modulus was measured in tension for eight flange specimens and four web specimens. The original load strain curves obtained for specimens X, Y, and Z are reproduced in Fig. 17. At this cross-section all three tensile specimens were loaded into the strain hardening range and the measurements necessary to determine the strain hardening characteristics were made.

Specimen Y was cut from the web of the section and exhibits the sharp upper yield point and significant strain hardening modulus usually associated with the structural steels. The modulus computed for this specimen was 680 ksi. On the other hand specimens X and Z exhibit a rather rounded knee and a reduced strain-hardening modulus. The areas of interest are emphasized

by the arrows in Fig. 17. Although the rounded knee of the load-strain diagram can be caused by influences other than cold-bending [22] it is gratifying to note the close agreement between the behavior predicted by the model used for Fig. 16 and the flange specimens of Fig. 17.

For the other cross-sections used in the investigation of [2], the results were similar. In each case where comparison was possible, the strain hardening modulus for the web specimen was approximately one third greater than the average for the flange specimens.

In summary, for sections which have been straightened by rotarizing, the effective material characteristics (assuming the flanges to exert the dominant influence) are those of a bilinear material having an effective value of E_{st} which is decreased from that measured for the virgin material. The effect of this process is to reduce the lateral and local buckling capacity of the member [17].

Tentatively, it appears that the stiffness reduction in certain portions of rotarized beams may be in the order of 25%. However, it should be noted that in the structural loading tests reported in [2], the member deformation capacity was sufficient for the frames tested to reach the predicted ultimate loads. In spite of the reduced stiffness of the material in the strain hardening range, local buckling did not occur until substantial deformations at the ultimate load were observed.

Studies should be initiated to define, in a statistical manner, the magnitudes of the curvature reversals which may be expected during rotarizing. Along with this data, a knowledge of the behaviour of the material when subjected to large reversals of strain is essential. Finally tests must be performed on members which have been rotarized in order to provide a check on the structural behaviour.

Summary and Conclusions

This report has examined the influence of the stress-strain characteristics of the material on moment redistribution in the inelastic range. In particular the important role played by the strain-hardening portion of the stress-strain curve has been emphasized.

It may be concluded that a definite strain hardening range is necessary to ensure moment redistribution. Within certain limits, the ideal material for a plastically designed structure is that which possesses a large value of E_{st} to ensure realistic limits on the flange plate geometry to preclude premature local buckling and, in addition, possesses a large value of ϵ_{st} to provide a large rotation capacity for a given yielded length.

The structural steels seem ideally suited for their role in plastic design since they posses the desired values of E_{st} and ϵ_{st}. For the structural steels, local buckling rather than material failure is the cause of rotation capacity termina-

tion. Fortunately, a high value of E_{st} leads to both a large local buckling capacity and an increase in the efficiency of moment redistribution.

Finally the report has examined the influence of the rotary straightening process on the effective material properties. It is concluded that the strain reversals produced by this process produce a decrease in the strain hardening modulus. This is supported by the results of coupon tests taken from rotarized members. No quantitative conclusions can be drawn, however, it is felt that the effect of the rotary straightening process explains the apparently reduced deformation capacity observed in some cases [2]. It is worthy of note that in spite of this reduction, the predicted ultimate loads were still reached. More research should be performed to fully determine the effect of rotarizing on structural behaviour.

Acknowledgements

This study is part of a general investigation "Plastic Design in High Strength Steel" in progress at Fritz Engineering Laboratory, Lehigh University. Dr. L. S. Beedle is Director of the Laboratory and Dr. L. W. Lu is the Project Director. The investigation is sponsored jointly by the Welding Research Council and the Department of the Navy, with funds furnished by the American Institute of Steel Concruction, American Iron and Steel Institute, Naval Ships Systems Command, and Naval Facilities Engineering Command. The Column Research Council acts in an advisory capacity.

Nomenclature

E modulus of elasticity
E_{st} strain hardening modulus
E_{st}^* effective strain hardening modulus (after cold bending)
I major axis moment of inertia
L length
M bending moment
M_p plastic moment capacity
M_0 maximum moment on member
P load
P_p load predicted by simple plastic theory
d depth of cross-section
v deflection
α proportionality constant (stress)
ϵ strain
ϵ_y yield strain ($\epsilon_y = \sigma_y/E$)
ϵ_{st} strain at onset of strain hardening

σ stress
σ_y yield stress
ϕ curvature
ϕ_p curvature corresponding to attainment of M_p, assuming ideally elastic behaviour ($\phi_p = M_p/EI$)
ϕ_{st} curvature at onset of strain hardening
τL Yielded length, that length over which M exceeds M_p

Bibliography

1. Adams, P. F., Lay, M. G. and Galambos, T. V.: Experiments on High Strength Steel Members, Welding Research Council Bulletin No. 110, November 1965.
2. Yura, J. A.: The Strength of Braced Multi-Story Steel Frames, Fritz Laboratory Report No. 273.28, September 1965.
3. Adams, P. F.: Plastic Design in High Strength Steel, Fritz Laboratory Report No. 297.19, Lehigh University, May 1966.
4. Beedle, L. S.: Plastic Design of Steel Frames, John Wiley & Sons Inc., New York, 1958.
5. Lay, M. G. and Galambos, T. V.: Inelastic Beams Under Moment Gradient, Proc. ASCE, ST 1, February 1967.
6. Yang, C. H.: The Plastic Behavior of Continuous Beams. Thesis presented to Lehigh University, Bethlehem, Pa., in 1951, in partial fulfillment of the requirements for the degree of Doctor of Philosophy.
7. Horne, M. R.: The Effect of Strain-Hardening on the Equalization of Moments in the Simple Plastic Theory, British Welding Research Association FE. 1 – Committee on Load Carrying Capacity of Frame Structures, September 1949.
8. Lay, M. G. and Smith, P. D.: Role of Strain-Hardening in Plastic Design Proc. ASCE, Vol. 91, ST 3, June 1965.
9. Adams, P. F. and Galambos, T. V.: Discussion of Importance of Strain-Hardening in Plastic Design, Proc. ASCE, Vol. 92, ST 2, April 1966.
10. Lay, M. G. and Galambos, T. V.: Inelastic Beams Under Moment Gradient, Proc. ASCE, Vol. 93, ST 1, February 1967.
11. Lay, M. G.: Flange Local Buckling in Wide-Flange Shapes, Proc. ASCE, Vol. 91, ST 6, December 1965.
12. Kerfoot, R. P.: Rotation Capacity of Beams, Fritz Laboratory Report No. 297.14, Lehigh University, March 1965.
13. Lukey, A. F.: Rotation Capacity of Wide Flange Beams Under Moment Gradient, M. Sc. Thesis, University of Alberta, Edmonton, Canada, May 1967.
14. Lay, M. G.: A New Approach to Inelastic Structural Design, Proc. ICE, London, England, May 1966.
15. Hrennikoff, A. P.: Importance of Strain-Hardening in Plastic Design, Proc. ASCE, Vol. 91, ST 4, August 1965.
16. Haaijer, G.: Plate Buckling in the Strain-Hardening Range, Proc. ASCE, Vol. 83, EM 2, April 1957.
17. Galambos, T. V.: Beams, Lecture Notes on Plastic Design of Multi-Story Frames, Chapter 3, Fritz Laboratory Report, 273.20, Lehigh University, 1965.
18. Ketter, R. L., Kaminsky, E. L. and Beedle, L. S.: Plastic Deformation of Wide-Flange Beam-Columns, Trans. ASCE, Vol. 120, 1955, Pp. 1028.

19. CHAJES, A., BRITVEC, S. J. and WINTER, G.: Effect of Cold-Straightening on Structural Sheet Steels, Proc. ASCE, Vol. 89, ST 2, April 1963.
20. LAY, M. G.: Discussion of Effect of Large Alternating Strains on Steel Beams, Proc. ASCE, Vol. 91, ST 4, August 1965.
21. FREUDENTHAL, A.: The Inelastic Behaviour of Engineering Materials and Structures, John Wiley & Sons, Inc., New York, N. Y., 1950.
22. BEEDLE, L.S. and TALL, L.: Basic Column Strength, Proc. ASCE, Vol. 86, ST 7, July 1960.

Summary

This report presents the results of a study of a three span beam. The study considered the spread of the yielded zones at "plastic hinge" locations by using a moment-curvature relationship which directly reflects the stress-strain curve of the material. The effect of the material properties on moment redistribution was investigated as well as the influence of the rotary cold-straightening process on the material properties.

Résumé

Ce rapport présente les résultats de l'étude d'une poutre à trois portées. L'étendue des zones influencées par l'emplacement de «charnières plastiques» est étudiée au moyen d'une parenté entre le moment et la courbure. Cette parenté illustre directement le diagramme des tensions et des efforts du matériel. Les effets des propriétés des matériaux sur la répartition des moments sont égalements étudiés ainsi que l'influence du procédé rotatif de redressement à froid sur les propriétés des matériaux.

Zusammenfassung

Dieser Beitrag zeigt die Ergebnisse einer Untersuchung an einem Dreifeldträger. Die Studie betrachtet die Ausdehnung der ausgewichenen Zonen im Bereiche des plastischen Gelenkes mittels einer Momenten-Durchbiegungs-Beziehung, die direkt auf der Spannung-Dehnungs-Kurve des Materials fußt. Die Wirkung der Materialeigenschaften auf die Momentenverteilung ist ebenso untersucht worden wie der Einfluß der Rotations-Kaltreckung auf die Materialeigenschaften.